Title

Curve shortening and the rendezvous problem for mobile autonomous robots

Journal

IEEE Transactions on Automatic Control, 52(6)

ISSN

0018-9286

Authors

Smith, Stephen L
Broucke, Mireille E.
Francis, Bruce. A.

Publication Date

2007-06-01

DOI

10.1109/TAC.2007.899024

Peer reviewed

$x_1(0)$ gets bigger (i.e., the initial distance of the ball to the center of the beam becomes larger) the quadratic term in the (11) becomes more significant which determines the value of the regulating signal in (12). In the case of approximate feedback linearization-based controller, we solve a linear equation to find the input signal, thus neglecting higher order terms, which may be the reason of losing the control power on larger neighborhoods of the origin.

We remark that, in [12], the authors proposed a nonlinear scheme to globally stabilize the ball and beam apparatus. In the current note, we only extend the existing linearization-based techniques to locally stabilize approximate feedback linearizable systems including the example described above.

V. Concluding Remarks

In this note, we introduced a new control algorithm for stabilizing nonlinear systems. The control algorithm presented in the note belongs to the family of sampled-data controllers. At each sampling interval, the input signal u is found by solving a polynomial equation in u. The polynomial coefficients are functions of the state at the sample time. The approach allows us to account for higher order terms normally neglected in stabilizing techniques based on system linearization. We illustrated our control scheme on the ball and beam apparatus and compared our controller to the well known approximate feedback linearization-based stabilizing controller.

References

[1] A. Isidori, *Nonlinear Control Systems*. London, U.K.: Springer-Verlag, 1995.

[2] J. Hauser, S. Sastry, and P. Kokotović, "Nonlinear control via approximate input-output linearization: The ball and beam example," *IEEE Trans. Autom. Control*, vol. 37, no. 3, pp. 392–398, Mar. 1992.

[3] K. K. Lee and A. A. Arapostathis, "Remarks on smooth feedback stabilization of nonlinear systems," *Syst. Control Lett.*, vol. 10, pp. 41–44, 1988.

[4] D. Aeyels, "Stabilizability of a class of nonlinear systems by a smooth feedback control," *Syst. Control Lett.*, vol. 5, pp. 289–294, 1985.

[5] R. W. Brockett, *Finite Dimensional Linear Systems*. New York: Wiley, 1970.

[6] E. D. Sontag, *Mathematical Control Theory*. New York: Springer-Verlag, 1990.

[7] F. H. Clarke, Y. S. Ledyaev, E. D. Sontang, and A. I. Subbotin, "Asymptotic controllability implies feedback stabilization," *IEEE Trans. Autom. Control*, vol. 42, no. 10, pp. 1394–1406, Oct. 1997.

[8] H. K. Khalil, "Performance recovery under output feedback sampled-data stabilization of a class of nonlinear systems," *IEEE Trans. Autom. Control*, vol. 49, no. 12, pp. 2173–2184, Dec. 2004.

[9] R. G. Buck, *Advanced Calculus*. New York: McGraw-Hill, 1965.

[10] M. Tham, "Mathematics of sampled data systems," in Study Notes Digit. Control, Chem. Process Eng., Univ. New Castle upon Tyne, 1996.

[11] C. Aguilar and R. Hirschorn, Report on Summer NSERC Research Project, Dept. Math. Statist., Queens Univ. Kingston, 2003, Stabilization of an Inverted Pendulum.

[12] C. Barbu, R. Sepulchre, P. Kokotovic, and W. Lin, "Global asymptotic stabilization of the ball-and-beam model," in *Proc. 36th IEEE Conf. Decision and Control*, Dec. 1997, pp. 2351–2355.

[13] J. Krener, "Approximate linearization by state feedback and coordinate change," *Syst. Control Lett.*, vol. 5, pp. 181–185, 1984.

Curve Shortening and the Rendezvous Problem for Mobile Autonomous Robots

Stephen L. Smith, *Student Member, IEEE*, Mireille E. Broucke, *Member, IEEE*, and Bruce A. Francis, *Fellow, IEEE*

***Abstract*—If a smooth, closed, and embedded curve is deformed along its normal vector field at a rate proportional to its curvature, it shrinks to a circular point. This curve evolution is called Euclidean curve shortening and the result is known as the Gage–Hamilton–Grayson theorem. Motivated by the rendezvous problem for mobile autonomous robots, we address the problem of creating a polygon shortening flow. A linear scheme is proposed that exhibits several analogues to Euclidean curve shortening: The polygon shrinks to an elliptical point, convex polygons remain convex, and the perimeter of the polygon is monotonically decreasing.**

***Index Terms*—Curve shortening, distributed control, mobile autonomous robots.**

I. Introduction

This note studies the *rendezvous problem* for mobile autonomous robots, in which the goal is to develop a local control strategy that will drive each robots's state (usually its position) to a common value. Research on this problem has been performed in both discrete time [1]–[7] and continuous time [8], [9]. The discrete time research can be split into synchronous systems [1]–[5] (i.e., each robot moves only at global clock ticks), and asynchronous systems [6], [7] (i.e., no global clock is present). In the synchronous case, there have been several papers on *circumcenter algorithms* [1]–[3], in which each robot moves towards the center of the smallest circle containing itself and every robot it sees. In both the continuous and discrete time cases, the research has assumed fixed communication topologies—the sensors are omnidirectional and have a range larger than their environment, allowing each robot to see all others—and time-varying or state-dependent communication topologies—the sensors have limited range; the sensors are directional; or, communication links may be dropped or added.

In this note, we look at the rendezvous problem from a different perspective. We are concerned with the shape of the formation of robots as they converge to their meeting point. We would like the formation to become more "organized," in some sense, as time evolves. We use a simple model, numbering the robots from 1 to n, and consider a fixed communication topology in continuous time. We then view the robot's positions as the vertices of a polygon, and, motivated by the Gage–Hamilton–Grayson theorem described below, we seek to create an analogous polygon shortening flow.

To introduce the Gage–Hamilton–Grayson theorem, consider a smooth, closed curve $\mathbf{x}(p,t)$ evolving in time: $p \in [0,1]$ parameterizes the curve; $t \geq 0$ is time; and $\mathbf{x}(p,t) \in \mathbb{R}^2$. We can evolve this curve along its inner normal vector field $\mathbf{N}(p,t)$ at a rate proportional

Manuscript received September 20, 2005; revised May 22, 2006 and February 16, 2007. Recommended by Associate Editor I. Kolmanovsky. This work was supported in part by the Natural Sciences and Engineering Research Council of Canada (NSERC).

S. L. Smith is with the Department of Mechanical Engineering, University of California, Santa Barbara, CA 93106 USA (e-mail: stephen@engineering.ucsb.edu).

M. E. Broucke and B. A. Francis are with the Department of Electrical and Computer Engineering, University of Toronto, ON M5S 3G4 Canada (e-mail: broucke@control.utoronto.ca; bruce.francis@utoronto.ca).

Digital Object Identifier 10.1109/TAC.2007.899024

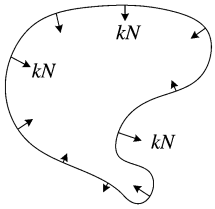

Fig. 1. Euclidean curve shortening flow.

to its curvature $k(p,t)$ (curvature is the inverse of the radius of the largest tangent circle to the curve at $\mathbf{x}(p,t)$, on the concave side)

$$\frac{\partial \mathbf{x}}{\partial t}(p,t) = k(p,t)\mathbf{N}(p,t). \tag{1}$$

This curve evolution is known as the *Euclidean curve shortening* flow [10], and is depicted in Fig. 1. Let $L(t)$ and $A(t)$ denote respectively the length and enclosed area of the curve at time t. Gage [11]–[13], Hamilton [13], and Grayson [14], [15] showed that a smooth, closed and embedded curve evolving according to (1) remains embedded and shrinks to a circular point. The term "circular point" means that the curve collapses to a point and, if we zoom in on the curve as it is collapsing, the curve is becoming circular. Throughout the evolution, $\dot{A}(t) = -2\pi$ and $L(t)$ is monotonically decreasing. In [15] it is also stated that under (1), "the curve is shrinking as fast as it can using only local information." This notion will be clarified later.

There has been prior work in creating polygon shortening flows. Motivated by the curve shortening theory and applications in computer vision, Bruckstein *et al.* [16] study the evolution of planar polygons in discrete time. A scheme is proposed that shrinks polygons to elliptical points (the vertices collapse to a point, and if we zoom in on the collapsing polygon, the vertices are converging to an ellipse). In addition, [16] discusses a polygon shortening scheme based on the Menger–Melnikov curvature [17]. In [18], this scheme is studied and it is shown that most quadrilaterals shrink to circular points. In [19], a flow is formulated such that the area enclosed by the polygon shrinks at a rate of 2π and the perimeter of the polygon is monotonically decreasing.

In this note, we study a planar polygon in the complex plane, with vertices $z_1, \ldots, z_n$, as it evolves according to

$$\dot{z}_i = \frac{1}{2}(z_{i+1} - z_i) + \frac{1}{2}(z_{i-1} - z_i), \quad i = 1, \ldots, n \tag{2}$$

where the indices are evaluated modulo n. Thus, vertex i pursues the centroid (center of mass) of its two neighboring (according to numbering) vertices. A discrete-time version of (2) is studied in [16], and it is shown that the polygon shrinks to an elliptical point. The contributions of this note are as follows. We introduce the curve shortening theory and its relation to the rendezvous problem. We also demonstrate the importance of studying the shape of the formation of robots as they rendezvous. We then show the following under (2): 1) if vertices are arranged in a star formation about their centroid, they remain in a star formation for all time (in particular, the robots will not collide), 2) convex polygons remain convex, and 3) the perimeter of the polygon monotonically decreases to zero. Finally, we derive the optimal direction for shortening the perimeter of a polygon.

II. Polygon Shortening

We consider n robots in the plane to be the vertices of an n-sided polygon. In this section, we formally define a polygon and introduce two polygon shortening schemes.

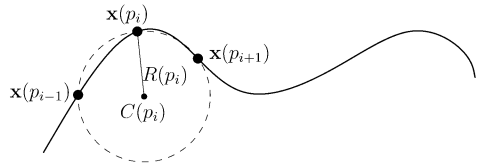

Fig. 2. Circumcenter for three points on the curve $\mathbf{x}(p)$.

A. Definition of an n-Gon

Following [20], we introduce the definitions of a polygon and a simple polygon in $\mathbb{R}^2$ (or equivalently $\mathbb{C}$). An *n-gon* (n-sided polygon) is a (possibly intersecting) circuit of n line segments $z_1z_2, z_2z_3, \ldots, z_nz_1$, joining consecutive pairs of n distinct points $z_1, z_2, \ldots, z_n$. The segments are called *sides* and the points are called *vertices*. A *simple* n-gon is one that is nonself-intersecting. We denote the counterclockwise *internal angle* between consecutive sides z_iz_{i+1} and $z_{i-1}z_i$ of an n-gon as β_i (as always, indices are modulo n). For a simple n-gon, these angles satisfy $\sum_{i=1}^{n} \beta_i = (n-2)\pi$. An n-gon is *convex* (*strictly convex*) if it is simple and its internal angles all satisfy $0 < \beta_i \leq \pi$ ($0 < \beta_i < \pi$).

B. Shortening by Menger–Melnikov Curvature

We now briefly describe the polygon shortening scheme studied in [16] and [18], and our reasons for not following this approach. Let $\mathbf{x}(p), p \in [0,1]$ be a smooth curve. Consider a set of parameter values $p_1 < p_2 < \cdots < p_n$ and the corresponding discrete points $\mathbf{x}(p_i)$. By connecting these points, we create an n-gon. As $n \to \infty$ and if the parameter values $\{p_i\}$ become dense in $[0,1]$, the n-gon converges to the smooth curve $\mathbf{x}(p)$. The idea is to create a polygon shortening scheme so that as $n \to \infty$, the scheme tends to (1).

If three consecutive points $\mathbf{x}(p_{i-1}), \mathbf{x}(p_i), \mathbf{x}(p_{i+1})$ are not collinear, there exists a unique circle (the *circumcircle*) that passes through them. Denote the radius of the circle by $R(p_i)$ and the center of this circle by $C(p_i)$, as shown in Fig. 2. The quantity $1/R(p_i)$ is called the *Menger–Melnikov curvature* and has the property that

$$\lim_{p_{i-1}, p_{i+1} \to p_i} \frac{1}{R(p_i)} = |k(p_i)|.$$

In addition, as the points $\mathbf{x}(p_{i-1})$ and $\mathbf{x}(p_{i+1})$ approach $\mathbf{x}(p_i)$, the quantity $(C(p_i) - \mathbf{x}(p_i))/R(p_i)$ approaches $\mathbf{N}(p_i)$ if $k(p_i) > 0$ and $-\mathbf{N}(p_i)$ if $k(p_i) < 0$. Therefore, we have

$$\lim_{p_{i-1}, p_{i+1} \to p_i} \frac{C(p_i) - \mathbf{x}(p_i)}{R(p_i)^2} = k(p_i)\mathbf{N}(p_i).$$

The Menger–Melnikov flow is then given by

$$\dot{\mathbf{x}}(p_i) = \frac{C(p_i) - \mathbf{x}(p_i)}{R(p_i)^2}, \quad i = 1, \ldots, n.$$

This flow was studied in [16] and [18]. However, due to the complexity of the system, the results are quite limited [16]. In [18], it is shown that a simple n-gon collapses to a point in finite time, and for $n = 4$, most quadrilaterals tend to regular polygons. However, when n is small, this flow may yield a poor approximation of the inner normal vector. In fact, for a convex n-gon, the approximation to the normal vector may not even point into the interior of the n-gon. Also, as the polygon collapses, the velocities of the vertices approach infinity, which is not ideal for our application. In light of these remarks, we propose the scheme presented next.

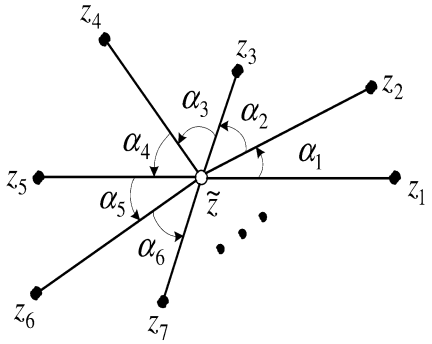

Fig. 3. Counterclockwise star formation.

C. Linear Scheme

The linear polygon shortening scheme is given by (2). Defining the aggregate state $z = (z_1, \ldots, z_n)$, where $z_i \in \mathbb{C}$, we get the simple form $\dot{z} = Az$. By exploiting the circulant structure of the matrix A, one can easily show the following properties.

Lemma 1: The polygon shortening scheme in (2), which can be written in the form $\dot{z} = Az$, has the following properties.

1) The eigenvalues of A are real, with one eigenvalue at zero, and all others on the negative real line.
2) The centroid $\tilde{z} := \sum_{i=1}^{n} z_i/n$ is stationary throughout the evolution.
3) The robots asymptotically converge to this stationary centroid.

The following theorem characterizes the geometrical shape of the points $z_i(t)$ as they converge to their centroid and is proved for discrete time in [16], and for general circulant pursuit in [21].

Theorem 2: Consider n points, $z_1(t), \ldots, z_n(t)$ evolving according to (2). As $t \to \infty$ these points converge to an ellipse. That is, $z_1(t), \ldots, z_n(t)$ collapse to an elliptical point.

III. Invariance of Formations

We now examine two classes of robot formations, star formations and convex formations, and show they are invariant under (2).

A. Star Formations Stay Star Formations

Consider our system of n robots, whose positions, not all collinear, are denoted by $z_1, \ldots, z_n$. Let $\tilde{z}$ be the centroid of these positions and r_i be the distance from the centroid to z_i. Let α_i denote the counterclockwise angle from $\tilde{z}z_i$ to $\tilde{z}z_{i+1}$ for $i = 1, \ldots, n$, modulo n. Then a star formation can be defined as follows.

Definition 3: (Lin et al. [8]): The n points are arranged in a *counterclockwise star formation* if $r_i > 0$ and $\alpha_i > 0$, for all $i = 1, \ldots, n$, and $\sum_{i=1}^{n} \alpha_i = 2\pi$. They are arranged in a *clockwise star formation* if $r_i > 0$ and $\alpha_i < 0$, for all $i = 1, \ldots, n$, and $\sum_{i=1}^{n} \alpha_i = -2\pi$.

This formation is shown in Fig. 3. In what follows, we will consider only counterclockwise star formations, since the treatment for clockwise star formations is analogous. Also, the case $n = 2$ is trivial, so it is omitted.

To determine whether a group of robots is in a star formation, we require a tool for measuring angles. This tool is given in Lemma 4. For $z \in \mathbb{C}$, let $\Re\{z\}$, $\Im\{z\}$ and $\bar{z}$ denote the real part, imaginary part, and complex conjugate of z, respectively.

Lemma 4 (Lin et al. [8]): Let z_1, z_2, and z_3 be three points in the complex plane, as shown in Fig. 4. Let $r_1 := |z_1 - z_2|$, $r_2 := |z_3 - z_2|$ and

$$F = \Im\{\overline{(z_1 - z_2)}(z_3 - z_2)\}.$$

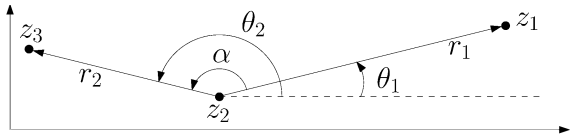

Fig. 4. Setup for the definition of the function F.

Then 1) $0 < \alpha < \pi, r_1 > 0$, and $r_2 > 0$ if and only if $F > 0$; 2) $\pi < \alpha < 2\pi, r_1 > 0$, and $r_2 > 0$ if and only if $F < 0$; 3) the points are collinear if and only if $F = 0$.

We are now ready to state the main theorem of this section.

Theorem 5: Suppose that n distinct points, with $n > 2$, are initially arranged in a counterclockwise star formation. If these points evolve according to (2), they will remain in a counterclockwise star formation for all time.

The proof uses the following two results.

Lemma 6 (Lin et al. [8]): Suppose that n distinct points, $z_1, \ldots, z_n$, with $n > 2$, are in a counterclockwise star formation. Then $\alpha_i < \pi, \forall i$.

Lemma 7 (Lin et al. [8]): If n points, $z_1, \ldots, z_n$ evolving according to (2) are collinear at some time t_1, then they are collinear for all $t < t_1$ and $t > t_1$.

Proof of Theorem 5: We begin by considering the function

$$F_i(t) = \Im\{\overline{(z_i(t) - \tilde{z})}(z_{i+1}(t) - \tilde{z})\} = r_i r_{i+1} \sin(\alpha_i).$$

By the definition of a counterclockwise star formation we have $r_i(0) > 0$ and $0 < \alpha_i(0) < \pi, \forall i$. Hence, by Lemma 4, $F_i(0) > 0, \forall i$. We want to show that $F_i(t) > 0, \forall i$ and $\forall t$, which by Lemma 4 shows that the vertices are in a counterclockwise star formation for all time.

Suppose by way of contradiction that t_1 is the first time that some F_i becomes zero. We can select $i = m$ such that $F_m(t_1) = 0$ and $F_{m+1}(t_1) > 0$, for if all the F_i's are zero at t_1, then the points are collinear, which by Lemma 7 is a contradiction. Hence, we have $F_i(t) > 0$ for all $t \in [0, t_1)$ and all i, $F_m(t_1) = 0$, and $F_{m+1}(t_1) > 0$.

Taking the time derivative of F_m, and noting that $\dot{\tilde{z}} = 0$ (see Lemma 1), we have $\dot{F}_m = \Im\{\overline{\dot{z}_m}(z_{m+1} - \tilde{z}) + \overline{(z_m - \tilde{z})}\dot{z}_{m+1}\}$.

By adding and subtracting $\tilde{z}$ in each term in (2) we can write (2) as

$$\dot{z}_i = \frac{1}{2}(z_{i+1} - \tilde{z}) + \frac{1}{2}(z_{i-1} - \tilde{z}) + (\tilde{z} - z_i).$$

Using this expression for $\dot{z}_m$ and $\dot{z}_{m+1}$ and simplifying, we obtain $\dot{F}_m = -2F_m + G_m$, where

$$\begin{aligned} G_m &= \frac{1}{2}\Im\{\overline{(z_{m-1} - \tilde{z})}(z_{m+1} - \tilde{z}) + \overline{(z_m - \tilde{z})}(z_{m+2} - \tilde{z})\} \\ &= \frac{1}{2}(r_{m-1} r_{m+1} \sin(\alpha_{m-1} + \alpha_m) \\ &\quad + r_m r_{m+2} \sin(\alpha_m + \alpha_{m+1})). \end{aligned} \tag{3}$$

Now, if $F_m(t_1) = 0$, by Lemma 4, one of the following four conditions must hold: 2) $\alpha_m(t_1) = \pi$ and $r_m(t_1), r_{m+1}(t_1) > 0$; 2) $\alpha_m(t_1) = 0$ and $r_m(t_1), r_{m+1}(t_1) > 0$; 3) $r_m(t_1) = 0$; 4) $r_{m+1}(t_1) = 0$.

Condition 4) cannot hold since $F_{m+1}(t_1) > 0$. Condition 1) cannot hold, for if it did, all points would lie on, or to one side of, the line formed by z_{m+1} and z_m, a contradiction by either Lemma 6 or 7. Assume that condition 2) holds. Then $\alpha_m(t_1) = 0$, and from (3), we obtain

$$\begin{aligned} G_m(t_1) &= \frac{1}{2}(r_{m-1} r_{m+1} \sin(\alpha_{m-1}) + r_m r_{m+2} \sin(\alpha_{m+1})) \\ &= \frac{1}{2}\left(\frac{r_{m+1}}{r_m} F_{m-1}(t_1) + \frac{r_m}{r_{m+1}} F_{m+1}(t_1)\right). \end{aligned}$$

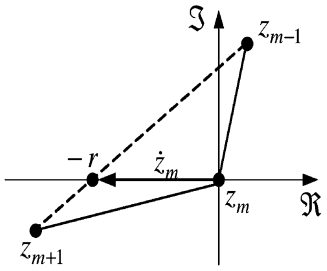

Fig. 5. Position of the points z_{m-1}, z_m, and z_{m+1} at $t = t_1$.

Since $r_m(t_1), r_{m+1}(t_1) > 0, F_{m+1}(t_1) > 0$, and $F_{m-1}(t_1) \geq 0$, it follows that $G_m(t_1) > 0$. By continuity of G_m, there exists $0 \leq t_0 < t_1$ such that $G_m(t) > 0$ for all $t \in [t_0, t_1]$. Also, by assumption, $F_m(t) > 0$ for $t \in [0, t_1)$. Therefore, $\dot{F}_m(t) = -2F_m + G_m > -2F_m$ for all $t \in [t_0, t_1)$. Integrating this and using the continuity of F_m, we obtain $F_m(t_1) \geq \mathrm{e}^{-2(t_1-t_0)} F_m(t_0) > 0$, a contradiction.

Finally, suppose condition 3) holds and $r_m(t_1) = 0$. Then $z_m(t_1)$ is positioned at the centroid, $\tilde{z}$. Assume without loss of generality that $\tilde{z} = 0$. Notice that if $z_i(t_1) = 0$, the angle $\theta_i(t_1)$ is not defined. We now establish that if $z_i(t_1) = 0$ and $\dot{z}_i(t_1) \neq 0$, then $\lim_{t \uparrow t_1} \theta_i(t)$ is well defined. Expanding z_i about t_1 we have $z_i(t_1) = z_i(t_1 - h) + h\dot{z}_i(t_1) + \mathcal{O}(h^2)$, where $\mathcal{O}(h^2)/h \to 0$ as $h \to 0$. If $z_i(t_1) = 0$ then $z_i(t_1 - h) = -h\dot{z}_i(t_1) + \mathcal{O}(h^2)$. Hence, $\lim_{h \to 0} z_i(t_1 - h)/h = -\dot{z}_i(t_1)$. Therefore, the limiting motion of $z_i(t)$ as $t \uparrow t_1$ is along the ray defined by $-\dot{z}_i(t_1)$. Because of this, we can define

$$\theta_i(t_1) := \begin{cases} \theta_i(t_1), & \text{if} \quad r_i(t_1) > 0 \\ \arctan\left(\frac{\Im\{-\dot{z}_i(t_1)\}}{\Re\{-\dot{z}_i(t_1)\}}\right), & \text{if} \quad r_i(t_1) = 0. \end{cases} \tag{4}$$

With this definition, we can talk about $\theta_i(t_1)$, and $\alpha_i(t_1)$, when $r_i(t_1) = 0$.

Suppose that by a rotation of the coordinate system, if necessary, the vector $z_{m+1}(t_1) + z_{m-1}(t_1)$ lies on the negative real axis. Then we can write

$$\frac{z_{m+1}(t_1) + z_{m-1}(t_1)}{2} = -r, \quad \text{where } r > 0. \tag{5}$$

We have $r > 0$ for if $r = 0$, then $z_{m-1}(t_1), z_m(t_1), z_{m+1}(t_1)$ all lie on a line through the centroid, and all other points must lie either on or to only one side of this line, implying that 0 is not the centroid, or all the points are collinear, both contradictions. Since $z_m(t_1) = 0$, from (2) and (5), we have $\dot{z}_m(t_1) = -r$, as shown in Fig. 5. If $n = 3$ then $z_m(t_1) = 0$ and the centroid of $z_{m+1}(t_1)$ and $z_{m-1}(t_1)$ is at $-r$, implying that 0 is not the centroid of the three points—a contradiction.

Therefore, we need only consider $n > 3$. Since $\dot{z}_m(t_1) = -r$, from (4), we obtain

$$\theta_m(t_1) = 0. \tag{6}$$

To obtain a contradiction for $n > 3$ we will show that (5) and (6) cannot both be satisfied. To do this, we consider two cases, $r_{m-1}(t_1) = 0$ and $r_{m-1}(t_1) > 0$. Since the points are in a star formation until t_1, we know that $\forall i$, $\alpha_i(t) \in (0, \pi)$ for $t \in [0, t_1)$. Hence, if $\theta_i(t_1)$ and $\theta_{i+1}(t_1)$ are defined via (4), then by continuity, $\alpha_i(t_1) \in [0, \pi]$.

If $r_{m-1}(t_1) = 0$, then from (5), we have $z_{m+1}(t_1) = -2r$. Therefore, $\theta_{m+1}(t_1) = \pi$, and from (6), $\theta_m(t_1) = 0$. However, this implies that all other $\theta_i(t_1)$'s that are defined must lie in $[-\pi, 0]$. Hence, $\Im\{z_i(t_1)\} \leq 0\ \forall i$, which implies that all points are collinear, or that 0 is not the centroid, both contradictions.

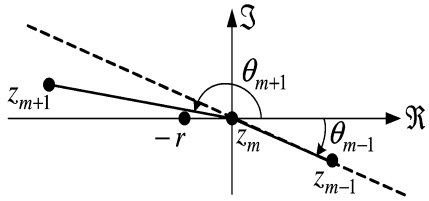

Fig. 6. Required geometry such that $\theta_{m-1}(t_1) \in [-\pi, 0], \theta_{m+1}(t_1) \in [0, \pi]$, and $z_{m+1}(t_1) + z_{m-1}(t_1) = -2r$. All points lie either on or to one side of the dotted line.

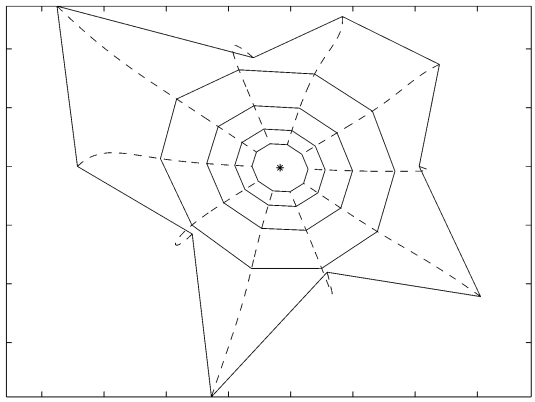

Fig. 7. Evolution of a polygon whose vertices are in a star formation about their centroid $*$. The dashed lines show the trajectories of each vertex.

If $r_{m-1}(t_1) > 0$ then from (6), and since $\alpha_m(t_1), \alpha_{m-1}(t_1) \in [0, \pi]$, we have that $\theta_{m+1}(t_1) \in [0, \pi]$ and $\theta_{m-1}(t_1) \in [-\pi, 0]$. So $\Im\{z_{m+1}(t_1)\} \geq 0$ and $\Im\{z_{m-1}(t_1)\} \leq 0$. Because of this, as can be verified in Fig. 6, for (5) to be satisfied either $z_{m-1}(t_1)$ and $z_{m+1}(t_1)$ are both real, in which case $\theta_{m+1}(t_1) - \theta_{m-1}(t_1) = \pi$, or neither is real and $\theta_{m+1}(t_1) - \theta_{m-1}(t_1) > \pi$. However, this implies that all points lie on, or to one side of, the line formed by $z_{m-1}(t_1)$. Thus, all points are collinear, or 0 is not the centroid, both contradictions. □

Fig. 7 shows the evolution of a polygon that is in a star formation about its centroid. Notice that the polygon remains in a star formation, becomes convex, and collapses to an elliptic point.

B. Convex Stays Convex

We now turn to the case where the formation is initially a convex n-gon.

Theorem 8: Consider a strictly convex n-gon at time $t = 0$, whose vertices z_i, $i = 1, \ldots, n$, are numbered counterclockwise. If these vertices evolve according to (2), the n-gon will remain strictly convex for all time.

The proof of this theorem is similar to that of Theorem 5; the reader may refer to [22] for a sketch or [23] for a full proof. Theorem 8 is analogous to convex curves remaining convex under (1), which is shown in [11].

A straightforward consequence of the theorem is the following.

Corollary 9: Consider an n-gon that is convex at $t = 0$. If the vertices evolve according to (2), then for any $t > 0$, the n-gon will be strictly convex.

Fig. 8 shows the evolution of an initially convex n-gon.

IV. Optimal Control Law for Perimeter Shortening

In [15], it is stated that a curve evolving according to (1) is shrinking as fast as it can using only local information. To see why and in

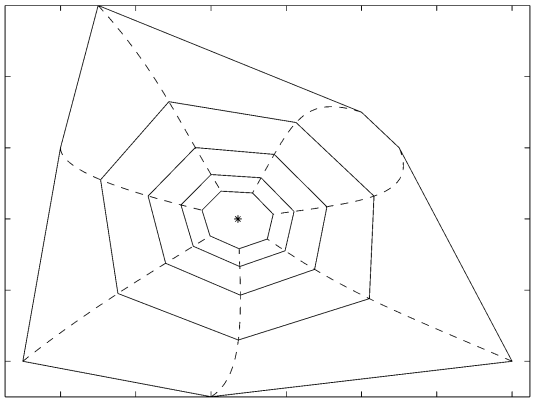

Fig. 8. Evolution of a convex n-gon. The solid lines show the trajectories of each vertex.

what sense this is true, reparametrize the curve in terms of its Euclidean arc-length s, defined via the differential arc-length element $ds := \|\partial \mathbf{x}/\partial p\| dp$. With this we can write the length of a curve as

$$L(t) = \int_0^{L(t)} ds = \int_0^1 \left\| \frac{\partial \mathbf{x}}{\partial p} \right\| dp. \tag{7}$$

To take the time derivative of this expression we differentiate $\|\partial \mathbf{x}/\partial p\|$ and obtain

$$\frac{\partial}{\partial t}\left\| \frac{\partial \mathbf{x}}{\partial p} \right\| = \frac{1}{\|\partial \mathbf{x}/\partial p\|} \left\langle \frac{\partial \mathbf{x}}{\partial p}, \frac{\partial}{\partial p}\frac{\partial \mathbf{x}}{\partial t} \right\rangle.$$

Substituting this into dL/dt and integrating by parts, we obtain

$$\frac{dL}{dt} = -\int_0^L \left\langle k\mathbf{N}, \frac{\partial \mathbf{x}}{\partial t} \right\rangle ds. \tag{8}$$

Therefore, the direction of $\partial \mathbf{x}/\partial t$ in which $L(t)$ is decreasing most rapidly is $\partial \mathbf{x}/\partial t = k\mathbf{N}$, which is the Euclidean curve shortening rule (1). Note that this flow is optimal only in the sense that the velocity of the curve at each point always points in the direction that maximizes the rate of decrease of $L(t)$.

We now give an analogous result for the discrete polygon case. Given an n-gon we can write its perimeter as

$$P(t) = \sum_{i=1}^{n} |z_{i+1} - z_i|. \tag{9}$$

To take the time derivative of $P(t)$ consider taking the derivative of $|z_{i+1} - z_i|^2 = \langle z_{i+1} - z_i, z_{i+1} - z_i \rangle$ (for $u, v \in \mathbb{C}^n, \langle u, v \rangle = u^* v$, where * denotes complex conjugate transpose). This yields

$$\begin{aligned} \frac{d}{dt}|z_{i+1} - z_i|^2 &= \frac{d}{dt}\langle z_{i+1} - z_i, z_{i+1} - z_i \rangle \\ &= 2\Re\left\{ \langle z_{i+1} - z_i, \dot{z}_{i+1} - \dot{z}_i \rangle \right\} \end{aligned}$$

but also, $(d/dt)|z_{i+1} - z_i|^2 = 2|z_{i+1} - z_i|(d/dt)|z_{i+1} - z_i|$. Combining these two expressions and letting $\dot{z}_i = u_i$, we obtain

$$\dot{P}(t) = \sum_{i=1}^{n} \Re\left\{ \left\langle \frac{z_{i+1} - z_i}{|z_{i+1} - z_i|}, u_{i+1} - u_i \right\rangle \right\}.$$

Since all indices are evaluated modulo n, this can be rewritten as

$$\dot{P}(t) = -\sum_{i=1}^{n} \Re\left\{ \left\langle \frac{z_{i-1} - z_i}{|z_{i-1} - z_i|} + \frac{z_{i+1} - z_i}{|z_{i+1} - z_i|}, u_i \right\rangle \right\}. \tag{10}$$

To maximize the rate of decrease of $P(t)$, u_i should point in the direction of $(z_{i-1} - z_i)/|z_{i-1} - z_i| + (z_{i+1} - z_i)/|z_{i+1} - z_i|$. This direction bisects the internal angle β_i of the n-gon. In general, neither the linear scheme (2) nor the shortening by Menger–Melnikov curvature points in this direction. However, this direction does not ensure that the polygon becomes circular (nor elliptical); in simulation, adjacent vertices may capture each other and the polygon may collapse to a line.

Using (10) and (2), we can determine $\dot{P}(t)$. For $\dot{P}(t)$ to be defined we require that adjacent vertices be distinct. This is ensured, for example, if the vertices start in a star formation about their centroid. The following result is analogous to the result in [11] that under (1), the length of the curve monotonically decreases.

Theorem 10: Consider an n-gon whose distinct vertices evolve according to (2). If adjacent vertices remain distinct, the perimeter $P(t)$ of the n-gon monotonically decreases to zero.

Proof: Substituting (2) into (10) and expanding we obtain

$$\begin{aligned} \dot{P}(t) = \frac{1}{2}\sum_{i=1}^{n} \Re\Big\{ &-|z_i - z_{i-1}| - |z_{i+1} - z_i| \\ &+ \left\langle \frac{z_i - z_{i-1}}{|z_i - z_{i-1}|}, z_{i+1} - z_i \right\rangle \\ &+ \left\langle \frac{z_{i+1} - z_i}{|z_{i+1} - z_i|}, z_i - z_{i-1} \right\rangle \Big\}. \end{aligned}$$

Each term in this summation has the form $\Re\{-|u| - |v| + \langle u/|u|, v\rangle + \langle v/|v|, u\rangle\}$. From the Cauchy-Schwarz inequality we have $\Re\{\langle u/|u|, v\rangle\} \leq |v|, \Re\{\langle v/|v|, u\rangle\} \leq |u|$, and, thus, $\Re\{-|u| - |v| + \langle u/|u|, v\rangle + \langle v/|v|, u\rangle\} \leq 0$. Therefore, $\dot{P}(t) \leq 0$. Equality is achieved if and only if $u/|u| = v/|v|$ for each term in the summation; that is, if and only if

$$\frac{z_i - z_{i-1}}{|z_i - z_{i-1}|} = \frac{z_{i+1} - z_i}{|z_{i+1} - z_i|}, \quad \forall i. \tag{11}$$

However, assume by way of contradiction that (11) is satisfied. Rotate the coordinate system such that z_1 and z_2 lie on the real axis and $z_2 - z_1 > 0$. Setting $i = 2$ in (11) we have $z_3 - z_2 > 0$, setting $i = 3$ we have $z_4 - z_3 > 0$, and so on. Hence, $z_{i+1} - z_i > 0, \forall i = 1, \ldots, n-1$, which implies that $z_n > z_1$. However, setting $i = n$ in (11) we have $z_1 - z_n > 0$, a contradiction. Therefore, (11) cannot be satisfied, $\dot{P}(t) < 0$, and since the vertices converge to their stationary centroid, $P(t)$ monotonically decreases to zero. □

V. Limitations of the Linear Scheme

There are two ways in which the linear scheme does not mimic Euclidean curve shortening. First of all, if an embedded curve is evolved via Euclidean curve shortening, its area is monotonically decreasing. However, for the linear scheme, in general, the area of a simple polygon is not monotonically decreasing. The second way in which the linear scheme does not mimic Euclidean curve shortening is in its effect on simple n-gons. If an embedded curve evolves according to the Euclidean curve shortening flow, it remains embedded. In contrast, a simple n-gon can become self-intersecting under the linear scheme. This topic is discussed in more detail in [23].

VI. Conclusion

In summary, under the simple distributed linear control law (2), the robots rendezvous and also become more organized, in the sense that the polygon becomes elliptical. Furthermore, star formations remain

so, convex polygons remain so, and the perimeter of the polygon decreases monotonically. These results are intended as a possible starting point for more useful behavior. As an example scenario, consider a number of mobile robots initially placed at random, and which should self-organize into a regular polygon (circle) for the purpose of forming a large-aperture antenna. Distributed control laws for this goal would have to be nonlinear. Research on this front is on-going.

Another topic for future research is to look at polygon shortening flows for wheeled robots which are subject to nonholonomic motion constraints.

Finally, drawing upon the results on curve shortening flows, there has been a similar development of curve expanding flows—If a smooth, closed, and embedded curve is deformed along its *outer* normal vector field at a rate proportional to the *inverse of its curvature*, it expands to infinity, and the limiting shape is circular [24]. Thus, a scheme for *deployment* of a fleet of mobile robots could be achieved by creating the analogous polygon expanding flow.

REFERENCES

[1] H. Ando, Y. Oasa, I. Suzuki, and M. Yamashita, "Distributed memoryless point convergence algorithm for mobile robots with limited visibility," *IEEE Trans. Robot. Autom.*, vol. 15, no. 5, pp. 818–828, May 1999.

[2] J. Cortés, S. Martínez, and F. Bullo, "Robust rendezvous for mobile autonomous agents via proximity graphs in arbitrary dimensions," *IEEE Trans. Autom. Control*, to be published.

[3] J. Lin, A. S. Morse, and B. D. O. Anderson, "The multi-agent rendezvous problem," in *Proc. IEEE Conf. Decision and Control*, Maui, HI, Dec. 2003, pp. 1508–1513.

[4] L. Moreau, "Stability of multiagent systems with time-dependent communication links," *IEEE Trans. Autom. Control*, vol. 5, no. 2, pp. 169–182, Feb. 2005.

[5] A. Jadbabaie, J. Lin, and A. S. Morse, "Coordination of groups of mobile autonomous agents using nearest neighbor rules," *IEEE Trans. Autom. Control*, vol. 48, no. 6, pp. 988–1001, Jun. 2003.

[6] L. Barriere, P. Flocchini, P. Fraigniaud, and N. Santoro, "Election and rendezvous in fully anonymous networks with sense of direction," *Theory Comput. Syst.*, 2005.

[7] P. Flocchini, G. Prencipe, N. Santoro, and P. Widmayer, "Gathering of asynchronous mobile robots with limited visibility," *Theoret. Comput. Sci.*, vol. 337, pp. 147–168, 2005.

[8] Z. Lin, M. Broucke, and B. Francis, "Local control strategies for groups of mobile autonomous agents," *IEEE Trans. Autom. Control*, vol. 49, no. 4, pp. 622–629, Apr. 2004.

[9] S. L. Smith, M. E. Broucke, and B. A. Francis, "A hierarchical cyclic pursuit scheme for vehicle networks," *Automatica*, vol. 41, no. 6, pp. 1045–1053, 2005.

[10] K.-S. Chou and X.-P. Zhu, *The Curve Shortening Problem*. New York: Chapman & Hall, 2001.

[11] M. E. Gage, "An isoperimetric inequality with applications to curve shortening," *Duke Math. J.*, vol. 50, no. 3, pp. 1225–1229, 1983.

[12] M. E. Gage, "Curve shortening makes convex curves circular," *Inventiones Math.*, vol. 76, pp. 357–364, 1984.

[13] M. E. Gage and R. S. Hamilton, "The heat equation shrinking convex plane curves," *J. Diff. Geom.*, vol. 23, pp. 69–96, 1986.

[14] M. A. Grayson, "The heat equation shrinks embedded plane curves to round points," *J. Diff. Geom.*, vol. 26, pp. 285–314, 1987.

[15] M. A. Grayson, "Shortening embedded curves," *Ann. Math.*, vol. 129, pp. 71–111, 1989.

[16] A. M. Bruckstein, G. Sapiro, and D. Shaked, "Evolution of planar polygons," *Int. J. Pattern Recognit. Artif. Intell.*, vol. 9, no. 6, pp. 991–1014, 1995.

[17] M. S. Mel'nikov, "Analytic capacity: Discrete approach and curvature of measure," *Sbornik: Math.*, vol. 186, no. 6, pp. 827–846, 1995.

[18] T. Jecko and J.-C. Leger, "Polygon shortening makes (most) quadrilaterals circular," *Bull. Kor. Math. Soc.*, vol. 39, no. 1, pp. 97–111, 2002.

[19] K. Nakayama, H. Segur, and M. Wadati, "A discrete curve-shortening equation," *Meth. Appl. Anal.*, vol. 4, no. 2, pp. 162–172, 1997.

[20] H. S. M. Coxeter, *Regular Polytopes*, 3rd ed. New York: Dover, 1973.

[21] J. A. Marshall, "Coordinated autonomy: Pursuit formations of multivehicle systems," Ph.D. dissertation, Univ. Toronto, Toronto, ON, Canada, 2005.

[22] S. L. Smith, M. E. Broucke, and B. A. Francis, "Curve shortening and its application to multi-agent systems," presented at the IEEE Conf. Decision and Control, Dec. 2005.

[23] S. L. Smith, M. E. Broucke, and B. A. Francis, Curve shortening and the rendezvous problem for mobile autonomous robots 2006 [Online]. Available: http://arxiv.org/abs/cs.RO/0605070, preprint. Available electronically at

[24] B. Chow and D. Tsai, "Geometric expansion of convex plane curves," *J. Diff. Geom.*, vol. 44, no. 2, pp. 312–330, 1996.

Frequency Response Functions for Nonlinear Convergent Systems

Alexey Pavlov, Nathan van de Wouw, and Henk Nijmeijer, *Fellow, IEEE*

***Abstract*—Convergent systems constitute a practically important class of nonlinear systems that extends the class of asymptotically stable linear time-invariant systems. In this note, we extend frequency response functions defined for linear systems to nonlinear convergent systems. Such nonlinear frequency response functions for convergent systems give rise to nonlinear Bode plots, which serve as a graphical tool for performance analysis of nonlinear convergent systems in the frequency domain. The results are illustrated with an example.**

***Index Terms*—Convergent systems, differential inclusions, frequency response functions, nonlinear systems, performance analysis.**

I. INTRODUCTION

A common way to analyze the behavior of a (closed-loop) dynamical system is to investigate its responses to harmonic excitations at different frequencies. For linear time invariant (LTI) systems, the information on responses to harmonic excitations, which is contained in frequency response functions, allows one to identify the system and analyze its properties such as performance and robustness. There exists a vast literature on frequency domain identification, analysis, and controller design methods for linear systems, see, e.g., [17] and [23]. Most (high-performance) industrial controllers, especially for motion systems, are designed and tuned based on these methods, since they allow one to analyze the performance of the closed-loop system. The lack of such methods for nonlinear systems is one of the reasons why nonlinear systems and controllers are not popular in industry. Even if a (nonlinear) controller achieves a certain control goal (e.g., tracking), which can be proved, for example, using Lyapunov stability methods, it is very difficult to conclude how the closed-loop system would respond to

Manuscript received March 1, 2006; revised October 24, 2006 and March 3, 2007. Recommended by Associate Editor D. Nesic. This work was supported in part by the Netherlands Organization for Scientific Research NWO and in part by the Research Council of Norway through the Strategic University Program CM-in-MC.

A. Pavlov is with the Department of Engineering Cybernetics, Norwegian University of Science and Technology, NO-7491, Trondheim, Norway (e-mail: alexey.pavlov@itk.ntnu.no).

N. van de Wouw and H. Nijmeijer are with the Department of Mechanical Engineering, Eindhoven University of Technology, 5600 MB Eindhoven, The Netherlands (e-mail: n.v.d.wouw@tue.nl; h.nijmeijer@tue.nl).

Digital Object Identifier 10.1109/TAC.2007.899020